The GALEX Catalog of UV Sources in the Magellanic Clouds

David Thilker, Luciana Bianchi, Raymond Simons

Center for Astrophysical Sciences, The Johns Hopkins University, Baltimore MD

Abstract

GALEX has performed unprecedented imaging surveys of the Magellanic Clouds (MCs) and surrounding areas including the Magellanic Bridge (MB) in near-UV (NUV, 1771-2831 Å) and far-UV (FUV, 1344-1786 Å) bands. Substantially more area was covered in the NUV than FUV, particularly in the bright central regions, because of the GALEX FUV detector failure. The 5σ depth of the NUV imaging varies between 20.8 and 22.7 (ABmag).

Our imaging *provides the first sensitive view of the entire content of hot stars in the Magellanic System, revealing the presence of young populations even in sites with extremely low star-formation rate surface density* like the MB, owing to high sensitivity of the UV data to hot stars and the dark sky in these bands.

Crowding limits the quality of source detection and photometry from the standard mission pipeline processing. Therefore, we performed custom PSF-fitting photometry of all GALEX exposures in the MC Survey region (<15° from the LMC, <10° SMC). The resulting catalog we have produced contains a few million unique NUV point sources. This poster provides an overview of the GALEX MCs Survey and highlights some of the science investigations that the catalog and imaging dataset are making possible.

Data + Coverage

GALEX imaging has resolution of $\approx 4.2/5.3''$ (FUV/NUV). We include observations from all GALEX surveys (AIS, MIS, NGS, GI, etc., Martin et al., 2005). As a result we achieve maximal depth at any specific position of interest. The radial limits of our GALEX MCs Survey, as discussed above and shown in Fig. 1, encompass a contiguous area of sky including both Clouds, the entire Magellanic Bridge (MB), and some of the Magellanic Stream nearest to the galaxies.

GALEX observation of any given field were frequently performed with separate exposures (visits). Exposures of the same field are later coadded to boost S/N. In Fig.2 we show the total accumulated exp. across the MC system.

The photometry was performed on single visit images of each pointing, and then merged into a catalog of unique sources (i.e., combining repeated measurements of the same source). This choice (rather than measuring on a coadd mosaic) allows us to track variability of sources if present, for those areas of the sky observed more than once, and to achieve more accurate photometry by PSF modeling per exposure.

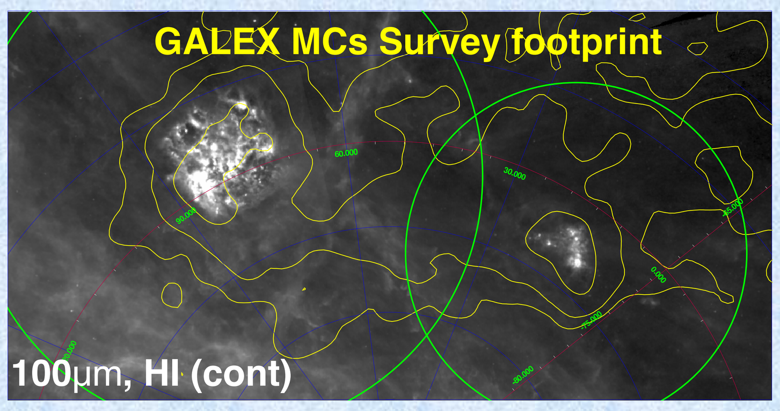

Figure 1: The GALEX Magellanic Clouds Survey region as seen by IRAS at 100 μm,with contours of the HI distribution of Putman et al. (1998). The N(HI) contours are drawn at 10^{19}, 10^{20} and 10^{21} cm^{-2}. We indicate radial limits of MC-specific GALEX analysis with green circles.

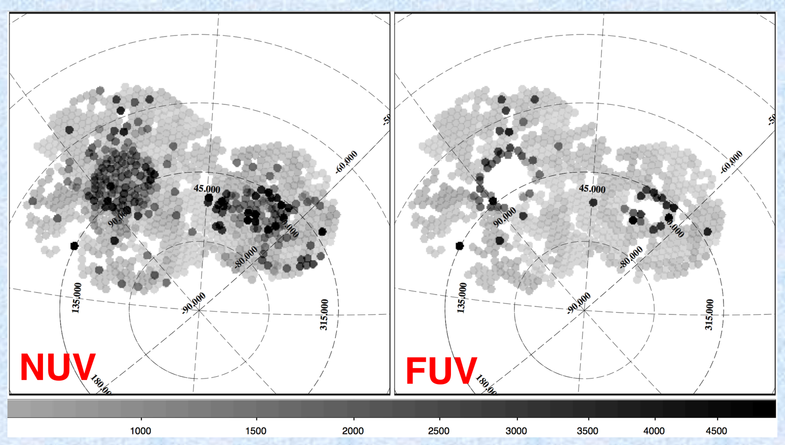

Figure 2: Total accumulated exposure time as a function of position for the NUV (left) and FUV (right), over the entire GALEX MCs Survey footprint.

Band	N(visits)	Max, Median Visit Exptime	Total Survey Exposure
NUV	2710	1705s, 107s	813ks
FUV	1828	1705s, 104s	376ks

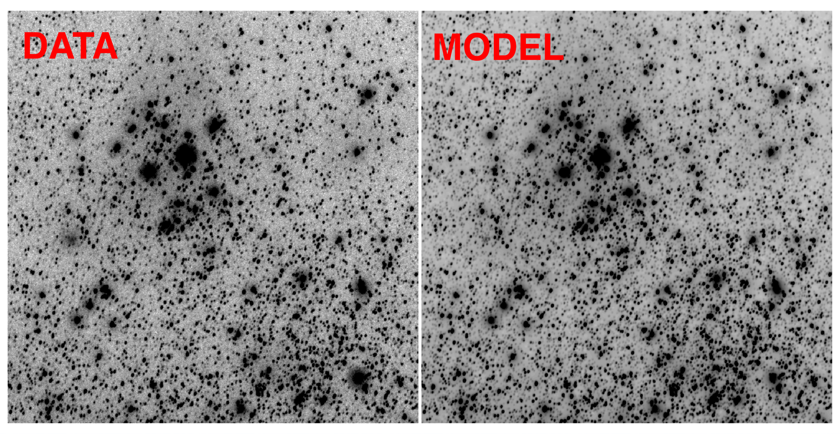

Figure 3: Comparison of observation (left) versus PSF-fitting model (right) for one small (0.4 kpc) SMC subregion. The determined background model has been added to the right panel. The model image retains all detections, even those which will not pass the eventual error cut. For this visit of 619 sec exposure the faintest sources detected have NUV~22.7, whereas those with err < 0.5 mag are limited to NUV~22.4 ABmag. In the full image we detect 3.4x the # of pipeline sources, using identical QA cuts.

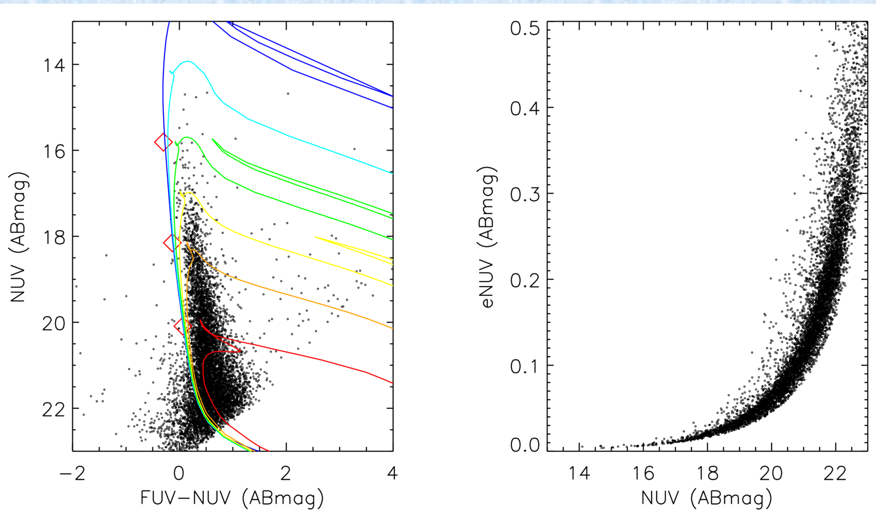

Figure 4: (left) Example CMD for one MIS-depth visit (1594 sec) in the SMC, retaining only sources with error <0.5 mag. The width of the main sequence is genuine, as shown by a magnitude-error plot (right). This suggests significant differential reddening in the field, such as can be measured with our SED fitting of UV-optical matched photometry. On left, we overplot Padua isochrones for log age[yr] = 7.0, 7.3, 7.7, 8.0, 8.3, 8.7 and models for MS stars (10, 5, and 3 M$_\odot$).

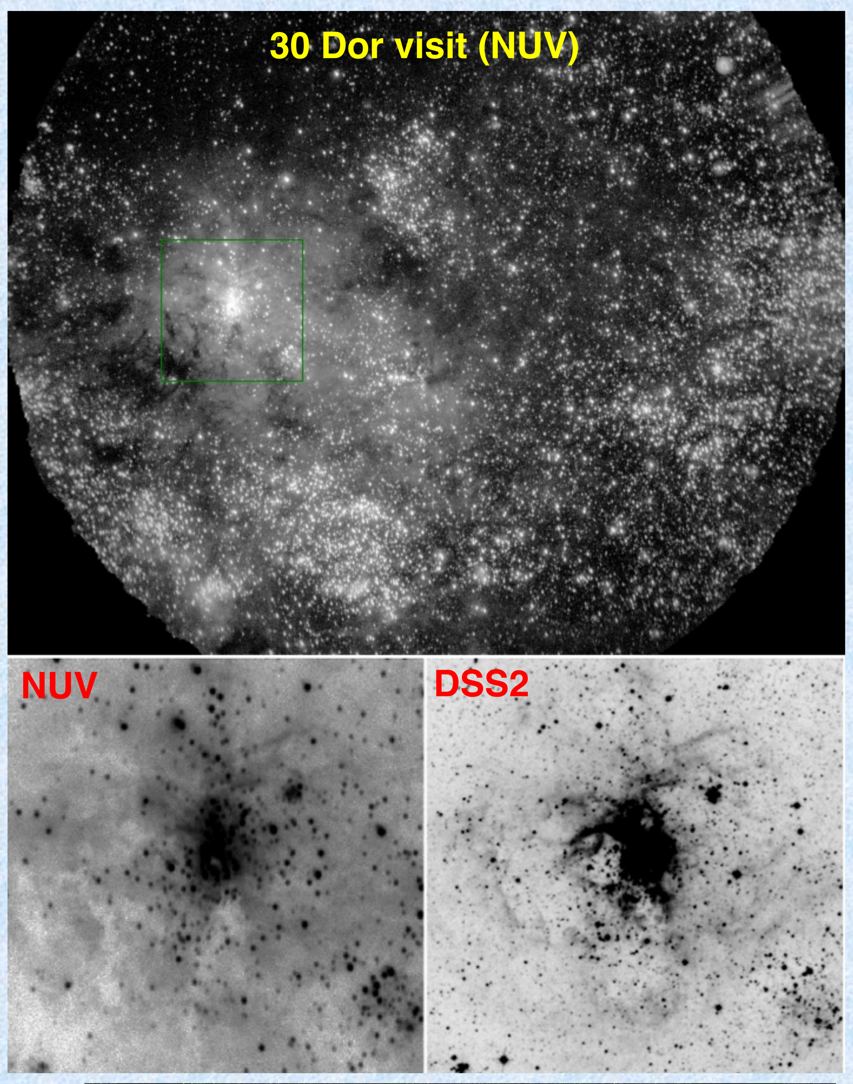

Figure 5: One GALEX field containing 30 Doradus and its environment. A close up view in the UV (left) and optical (right) is provided in the inset, and the location of this 0.2° (174 pc) box is marked in the wide-field image. The NUV image prominently displays the presence of dust, via bright regions of scattered light and also in absorption features

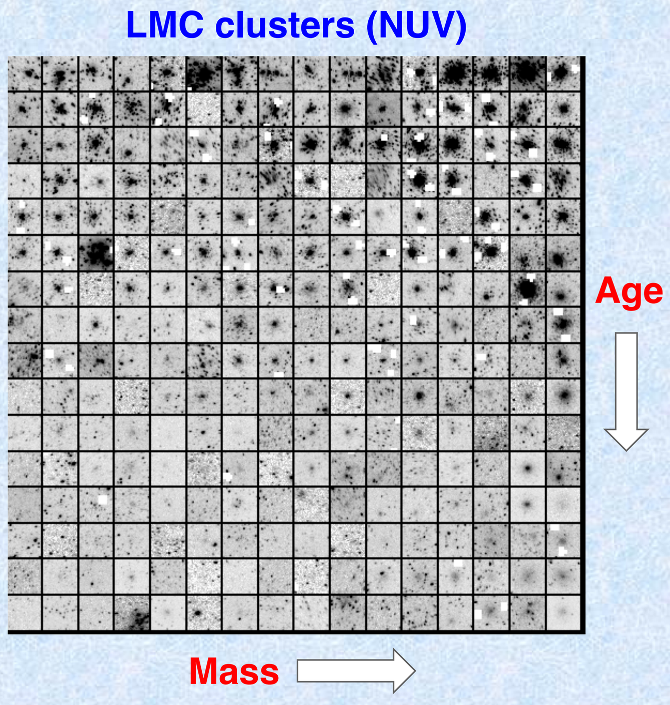

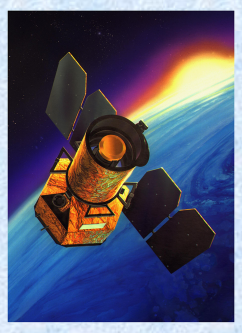

Figure 6: NUV images for 256 LMC clusters selected from Baumgardt et al. (2013). These are arranged such that the age increases downward and (within a row) the mass increases to the right. The field of view shown for each cluster is 38 pc.

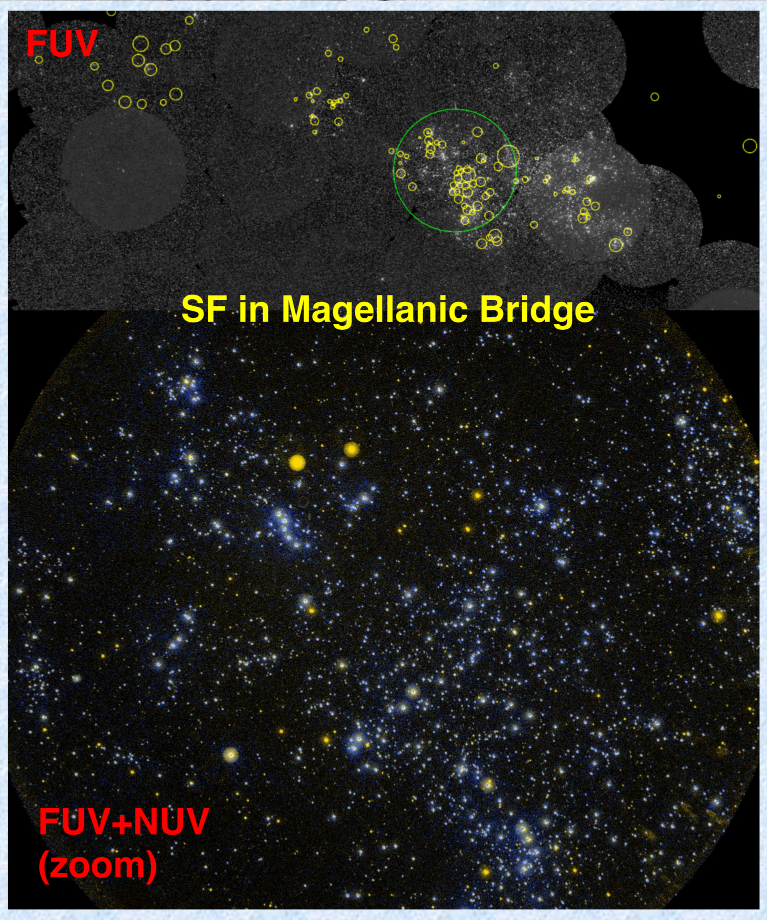

Figure 7: A view of the Magellanic Bridge from GALEX. (top) FUV imaging for several visits, demonstrating the detection of recent SF even outside the known OB associations (Bica & Schmitt, 1995, yellow circles). (bottom) FUV, NUV (blue/yellow) color image for one selected tile ~1.1 kpc in diameter and indicated with green in the top panel.

Young clusters, SF complexes

In addition to the resolved sources which constitute the current catalog, all young stellar clusters are detected in our UV images throughout the Magellanic System, including both Clouds and the Bridge. For each known cluster we extracted a GALEX cutout image. Non-cluster sources are being PSF-subtracted, allowing measurement of integrated NUV, FUV (when available) magnitudes. Our photometry of extended sources will be published separately. With existing measurements at longer wavelengths, these will be used to characterize cluster mass, extinction, and age using stochastic models for the low mass regime (following Krumholz+15).

In Fig. 5, to illustrate an extreme cluster environment, we show the GALEX observations of the starburst complex 30 Dor, comparing NUV and optical imaging in the inset. In Fig. 6 we display many clusters with more typical masses in the LMC sample (NUV only). In Fig. 6 it is apparent that the characteristic UV luminosity and morphology of the clusters varies as a function of both age and mass, while luminosity must also be modulated by local reddening.

Our images (Fig. 7) show that *the Western MB has a significant component of recent star formation unrepresented by the OB association catalog of Bica and Schmitt (1995).* We are studying the age-dependent hierarchical clustering behavior of SF in this low density environment, contrasting results versus similar metrics in the dense, inner portions of the MCs.

UV-optical SED fits

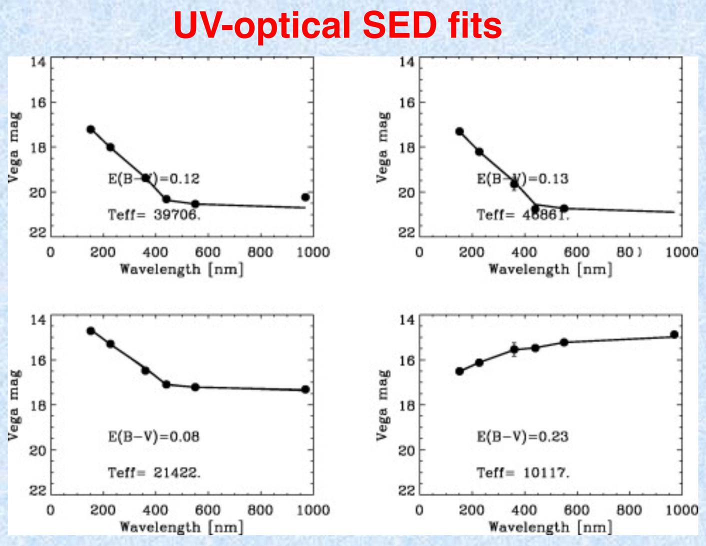

Figure 8: UV-optical photometry of example stars in the GALEX catalog with existing optical data from the MCPS Zaritsky et al. (2004). Dots are the photometric measurements, plotted at the λ_{eff} of the respective bandpasses, the best-fit model magnitudes are connected by a line. Errors are smaller than the symbol size, with a few exceptions seen in the two righthand panels. The derived T_{eff} and $E(B\text{–}V)$ are indicated.

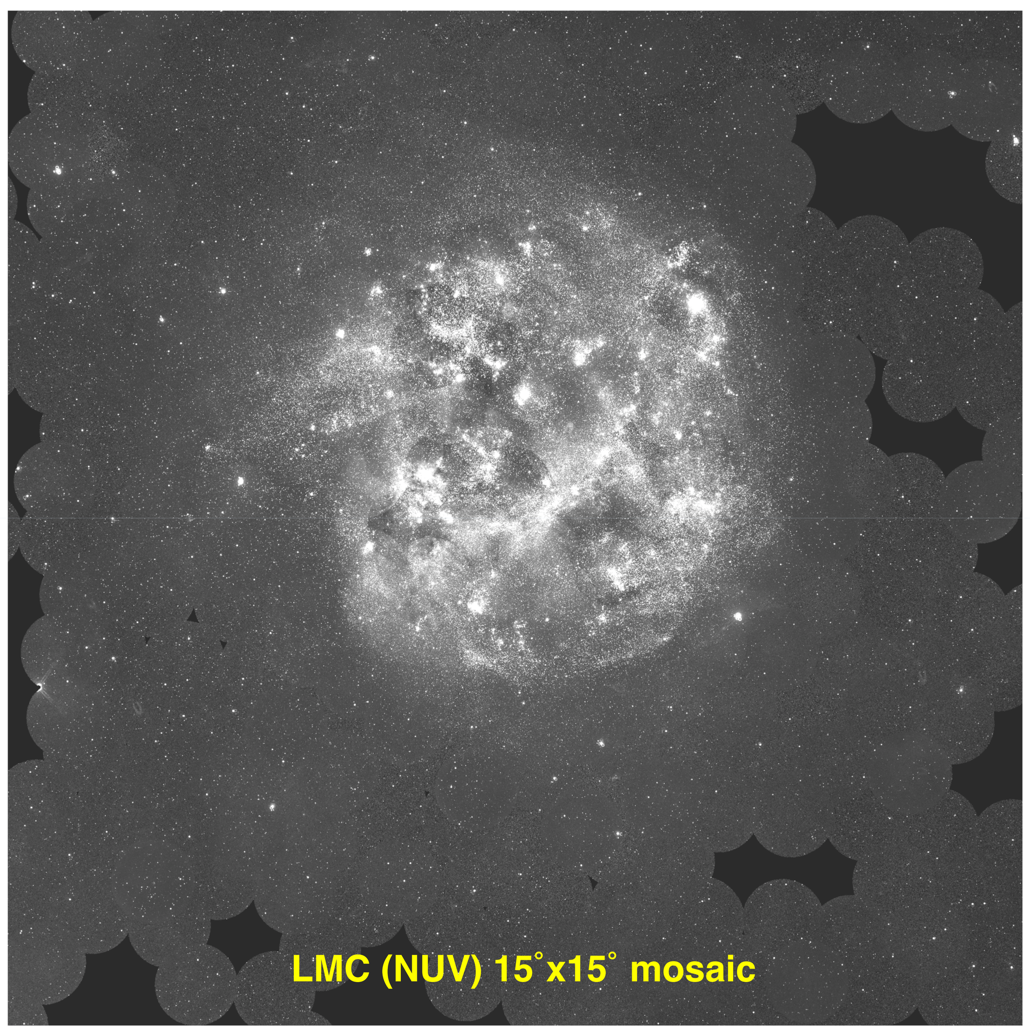

Figure 9: Mosaic of GALEX NUV imaging data for the LMC. We are now working on a superior coadd stack for both MCs with detailed background matching and iterative artifact rejection. The apparent LMC UV diameter is >10°, with a faint resolved component reaching well beyond - consistent with deep optical studies.

The UV source catalog

The GALEX pipeline based on Source Extractor (Bertin & Arnouts 1996) sometimes fails to resolve closely neighboring point sources in crowded fields. A more sophisticated PSF-fitting approach is required for photometry in dense fields with close and overlapping sources. The GALEX PSF varies slightly from visit to visit and slightly as a function of position within the field (Morrissey et al., 2007). We sought to account for this variation by determining the PSF core structure per visit, yet retaining information on the large scale PSF profile (FUV and NUV separately) from a mission-wide measurement supplied by the GALEX project (www.galex.caltech.edu/researcher/techdoc-ch5.html#2). Slight PSF ellipticity is noted in individual visits, especially for data taken in the late part of the mission. Variation of the PSF across a single tile (at least inside a radius of 0.55°) was not as significant as intra-visit changes.

We constructed a pipeline based on the IDL Starfinder package (Diolaiti+2000) with modifications/additions to handle the photon counting images from GALEX, especially in the case of short (AIS-depth) exposures for which many pixels can receive zero counts. We first detected stars with the mission-average PSF. We subtracted all stars from the input image, masked stellar residuals, and used a variant on the method of Hoversten+2011 to initially estimate the background emission. Results of the first detection run also identified sources that were both bright and isolated enough to represent the PSF. All neighbor stars within $150''\text{x}150''$were PSF-subtracted and background was removed, allowing the visit's PSF to be measured via an error-weighted stack of PSF stars. This PSF was blended with the mission-avg PSF outside of its central core. Photometry was then iteratively recomputed with increasing depth, refining the empirical PSF every iteration. After three iterations, the PSF solution is stable and we compute one last background model prior to a maximally deep, final PSF-fit run. As expected, we find that custom-PSF fitting better recovers simple aperture photometry for isolated sources compared to the mission PSF run, and importantly deblends crowded sources very well. With this method, photometry is first conducted blindly on NUV and FUV images separately, and a subsequent run of Starfinder finally attempts recovering as many NUV-detected sources in the FUV as possible by using the NUV positions as a prior. See Figs. 3 and 4 for example visit-level photometry products.

After performing photometric measurements for sources detected in each visit, we had a database containing multiple detections of astrophysically unique sources due to the overlap of adjacent tiles and also stemming from repeated visits. To produce a catalog of unique UV sources: (1) we first applied quality cuts on the concatenated source list, removing detections farther than 0.55° from the field center or lying in a region flagged as an artifact by the GALEX pipeline, (2) we then identified sources having repeated measurements within $2.5''$ separation, (3) for each set of coincident detections, the one having the highest exposure time was retained, except in comparatively rare cases of equal exp for which the source positioned closest to its field center was kept, (4) photometry measurements from multiple detections of each unique source were averaged with weighting, (5) finally a significance cut was applied to retain all unique sources having NUV error less than 0.5 mag. The final point source catalog of a few million entries contains measured positions/uncertainties, PSF magnitudes/errors, diffuse background levels, plus reference to the individual detections prior to the merge. The exact number depends on the choice of flag values rejected in step (1).

SED-fitting of resolved stars + future optical surveys

GALEX LMC sources with FUV and NUV photometry, and single optical counterparts (at U B V I) from the MCPS, were analyzed with grids of stellar model atmospheres, reddened progressively assuming a variety of extinctions curves (see Bianchi+2012a and Bianchi+2012b for details). The major parameters derived from SED fitting (through standard χ^2 minimization), are the stellar effective temperature T_{eff}, and the extinction towards the source, $E(B\text{–}V)$. The results depend on the assumed metallicity, and type of selective extinction ($A_\lambda/E(B\text{–}V)$); the latter may significantly vary across different environments. The UV fluxes are particularly sensitive to this parameter (e.g. Bianchi+2007 and Bianchi, 2011), and provide critical diagnostics for the hottest T_{eff}'s. Because the distance to the stars is known, once T_{eff} and $E(B\text{–}V)$ are derived we can also obtain an estimate of the radius (and therefore L_{bol}) by scaling the best-fit model to the observed fluxes, accounting for extinction. A few examples of stellar SED and best-fit models are shown in Fig. 8.

We plan to expand this work to include all regions of both Clouds, even areas with only NUV coverage, ideally making use of photometry from SMASH (Nidever+) and OGLE IV (Udalski+2015). Some of the candidate hottest, but low luminosity, sub-dwarf stellar populations that can be recovered with our observations are are too faint in optical bands for the currently available surveys. We plan to pursue deep optical imaging in critical blue bands (*u*, *g*) over the inner MCs (r<6° LMC, r<4 ° SMC, see Fig. 9), aiming for ABmag~26 as an 8σ limit.

References

Simons et al. (2013), J. Advances in Space Research, in press. http://dx.doi.org/10.1016/j.asr.2013.07.016

Bianchi et al. (2014) ApSS, 354, 103:112

Thilker et al. (2015) in prep., for final catalog

Visit catalogs on request now. Merged unique source catalog soon @ http://dolomiti.pha.jhu.edu/uvsky and MAST